IEEE Photonics Journal
An IEEE Photonics Society Publication

Open Access

Analysis of Spontaneous Raman and Rayleigh Scatterings in Distributed Fiber Raman Amplification Systems Based on a Random Distribution Model

Volume 9, Number 6, December 2017

Qiguang Feng
Wei Li
Liyan Huang

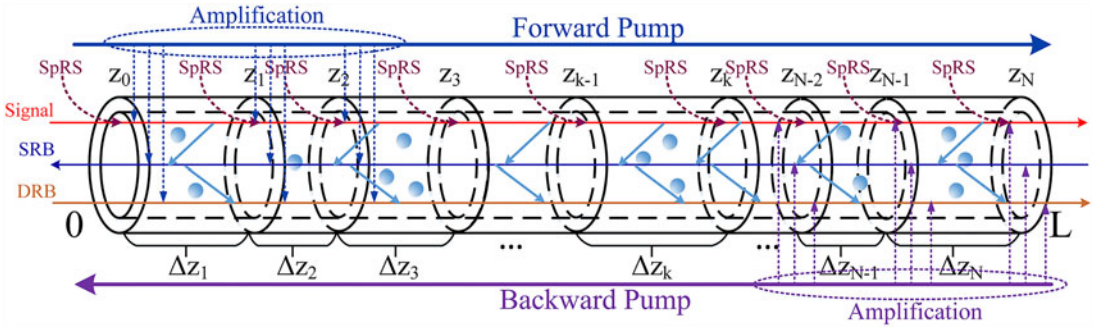

DOI: 10.1109/JPHOT.2017.2777475
1943-0655 © 2017 IEEE

IEEE photonics SOCIETY

IEEE

Analysis of Spontaneous Raman and Rayleigh Scatterings in Distributed Fiber Raman Amplification Systems Based on a Random Distribution Model

Qiguang Feng,[1] **Wei Li**,[1] **and Liyan Huang**[2]

[1]Q. Feng and W. Li are with the Wuhan National Laboratory for Optoelectronics, Huazhong University of Science and Technology, Wuhan 430074, China
[2]L. Huang is with Accelink Technologies Corporation Ltd., Wuhan 430205, China

DOI:10.1109/JPHOT.2017.2777475

Manuscript received October 12, 2017; revised November 17, 2017; accepted November 20, 2017. Date of publication November 22, 2017; date of current version December 14, 2017. This work was supported by China 863 project under Grant 2015AA017002. Corresponding author: Wei Li (e-mail: weilee@hust.edu.cn).

Abstract: The properties of light wave propagation with stochastic scattering in a fiber are particularly attractive because of their influence in various applications. Although stochastic scattering in fibers is of great significance, until now, no accurate theoretical model has described the randomness of the distributions and variations in scattering since the scattering sources are regarded as centralized or homogeneously distributed. In this paper, we proposed a model to analyze the random variation in scattering with time and location. Then, we employed the model to simulate stochastic scattering in distributed fiber Raman amplification (FRA) systems, including Rayleigh backscattering and spontaneous Raman scattering, which are crucial limitations of the distributed FRA systems. The simulations agreed well with our experimental measurements, proving that our model efficiently described stochastic scattering spectra and distributions in FRAs. Our theory accurately analyzed the distribution and evolution of scattering along the fiber and is a promising tool for optimizing the performance of distributed fiber systems, especially systems with distributed amplification such as fiber communication systems, random feedback fiber lasers, and fiber sensors.

Index Terms: Rayleigh backscattering (RB), spontaneous Raman scattering (SpRS), stimulated Raman scattering (SRS), fiber Raman amplification (FRA)

1. Introduction

The properties of light wave propagation with stochastic scattering in fibers are particularly attractive physical objects, because of their influence and applications in various engineering fields such as optical fiber telecommunications, fiber link monitoring, fiber lasers and fiber sensors. In recent years, the characteristics and application of random scattering in fiber have attracted significant attention from researchers [1]–[8]. Distributed fiber Raman amplifiers (FRAs) have become increasingly popular for long-haul fiber systems and long-reach unrepeated transmissions due to their lower noise figures compared with those of Erbium-doped fiber amplifiers (EDFAs) [1]–[4]. In distributed FRA systems, random double Rayleigh backscattering (DRB) and spontaneous Raman scattering (SpRS) are the main performance limitations. S. K. Turitsyn *et al.* demonstrated a novel random fiber laser, wherein Rayleigh backscattering (RB) provided randomly distributed feedback, and

stimulated Raman scattering (SRS) provided distributed amplifications [6]. The random RB is also important for fiber sensors, such as the distributed vibration sensor based on a phase-sensitive optical time domain reflectometry (Phi-OTDR) system [7].

In systems with distributed amplification, the randomly scattered light can be amplified, which more severely influences the system performance. A recurring challenge for the distributed FRAs is the presence of SpRS and DRB. SpRS can be randomly generated along the fiber and then amplified by the Raman pump light, whose characteristics are similar to the amplified spontaneous noise (ASE). Then, since no isolators are generally present in the distributed FRAs, the RB light is effectively amplified and generates considerable DRB light, which is amplified again by the Raman pump light [8], [9]. The amplified DRB light has the same wavelength and transmission direction as the signal and is partially coherent with the signal light. Thus, it can beat with the signal to induce multi-path interference (MPI) noise, thereby degrading the performance of the systems. In the few-mode FRAs, the amplified SpRS and Rayleigh scattering also clearly affect the gain and noise figure performance [11]. In ordinary fiber lasers, stimulated Rayleigh scattering induces a severe polarization mode instability [10]. In addition, in random feedback fiber lasers, the randomness of Rayleigh and Raman scattering determines the characteristics of the output light [12], [13]. Thus, in Phi-OTDR assisted by Raman amplification, RB and SpRS also severely limit measurement accuracy [14].

The analysis of random characteristics of scattering in fiber attracted a great deal of attention in the past [15]–[20]. In 1990, P. Gysel *et al.* investigated the spectral properties of RB light from single-mode fibers [15]. In 1996, P. Wan and J. Conradi analyzed the difference in scattering noise between systems employing distributed and lumped FRAs [16]. The model they employed generally assumed that RB and SpRS were homogeneously distributed additive Gaussian white noise [17], [18]. Recently, investigators have recognized that modeling the randomness of RB and SpRS distributions is an important area of study for random scattering in fiber. O. Okusaga *et al.* phenomenologically explained the influence of the random characteristics of RB based on guided entropy mode theory [17]. M. Fleyer *et al.* analyzed DRB noise considering the randomness of the RB coefficient in EDFA systems [18]. Regarding the randomness of SpRS, researchers have also reported a change in the spectrum of SpRS with the power of pump light [19]. Our group investigated the interaction of Rayleigh and Brillouin scattering and analyzed their influence in passive optical networks and fiber sensors [20].

According to these investigations, stochastic scattering was generally modeled as a centralized or homogeneously distributed noise, and only the random variation with time has been considered, which has led to noticeable differences between the primitive models and experimental results. Therefore, we proposed a random distribution model to analyze the randomness of scattering coefficients and distributions for stochastic scattering. In our model, both the random variations in the scattering electrical fields with time and scattering locations were considered. Then, we employed our model to analyze the characteristics of RB and SpRS in distributed FRAs to verify our theory since the stochastic RB and SpRS with Raman amplification were easier to measure precisely.

2. Theoretical Model

Fig. 1 presents the schematic diagram of random RB in the fibers. Photons propagating in a long fiber were coherently scattered by random refractive index inhomogeneities following Rayleigh's law. Most of the scattered photons leaked out of the fiber core. Only a few of them were backscattered and guided by the fiber. While the refractive index inhomogeneities were disordered, RB reflection coefficients varied randomly with time and locations, resulting in the randomness of the optical field of RB.

Fig. 2 presents a schematic diagram of a bi-directional pumped distributed FRA system and the DRB noise generation process in the system. Two pump waves coupled at the beginning and end of the fiber provided a distributed Raman gain along the fiber. The signal light was transmitted along the forward direction of the fiber and scattered randomly. Some of the backscattered

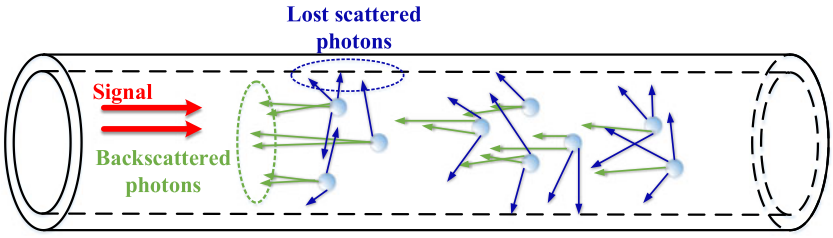

Fig. 1. Schematic diagram of random RB in fibers.

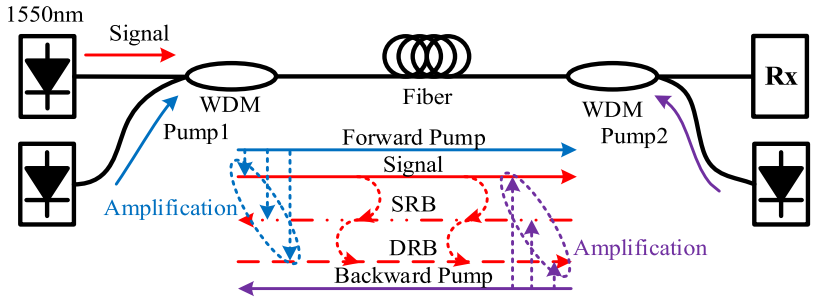

Fig. 2. Schematic diagram of a bi-directional pumped distributed FRA system and the DRB noise generation in the system.

guided photons generated a single Rayleigh backscattering (SRB) light. The SRB light was amplified by the Raman pump lights and backscattered randomly again to produce DRB light. The amplified DRB light was partially coherent with the signal light and interfered with the signal light. The DRB noise was the sum of several lights with different time delays in contrast with the signal light, which can be regarded as the stochastic MPI noise. In addition, when the two pump waves were transmitted along the fiber, the SpRS photons were generated, and the forward-guided photons were amplified. The SpRS noise characteristics changed with the pump power, and this noise was higher in intensity than the DRB noise [3], [4]. Thus, SpRS had more prominent impacts on the FRA system. The following section is our theoretical model and numerical method to address randomness in the DRB and SpRS noise.

First, we modeled the signal laser source using a quasi-monochromatic wave:

$$E_{in}(t) = E_0[1 + m(t)]\exp[j\varphi(t) + j\omega_0 t] \tag{1}$$

where $m(t)$ is the relative amplitude noise of the laser with a zero-mean autocorrelation function, $\varphi(t)$ is the laser phase noise, and ω_0 is the carrier frequency. The laser relative intensity noise (RIN) is defined as the Fourier transform of the autocorrelation function$\langle|E_{in}(t)|^2|E_{in}(t-\tau)|^2\rangle/\langle|E_{in}(t)|^2\rangle^2$, where $\langle\bullet\rangle$ is a time-average. The effect of polarization state variations during the propagation in a random birefringent fiber can be added by calculating the degree of polarization of the DRB field by using the properties of a Mueller matrix [21]. Hence, we used a scalar field in the following derivations, and we added the polarization effect by multiplying the calculated spectrum by a constant factor of 5/9.

According to earlier investigations [16]–[19], the RB sources uniformly distributed along the entire fiber, and the reflection coefficient $\gamma(z)$ with a unit (1/km) can be modeled as a complex white Gaussian zero-mean process. Assuming that the entire fiber length is L, the single and double back reflection locations are z_1 and z_2, respectively, the total DRB electrical field at the fiber output is

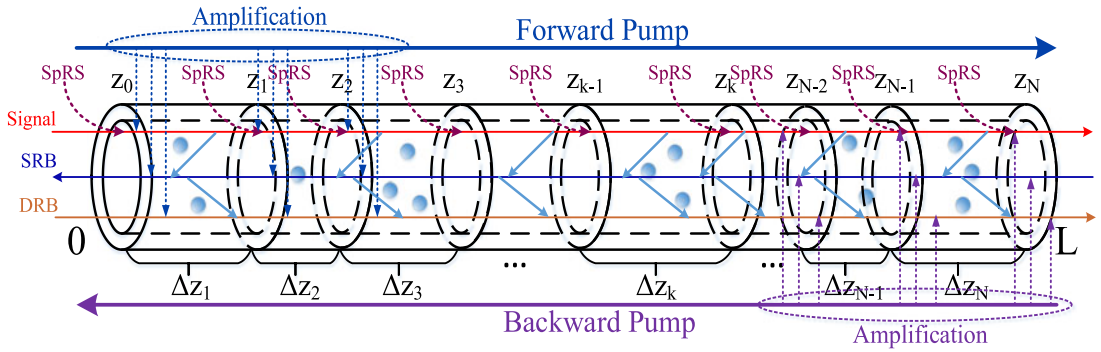

Fig. 3. Schematic diagram of the random distribution of the RB and SpRS sources locations.

given by

$$E_{DRB}(t) = \int_0^L dz_1 \int_0^{z_1} dz_2 T(z_2, z_1)\gamma(z_2) T(z_1, z_2)\gamma(z_1) \times T(0, L) E_{in}(t - nL/c - 2n(z_1 - z_2)/c) \quad (2)$$

where n is the fiber refractive index, c is the speed of light in vacuum, and $T(z_i, z_j)$ is the transform function of the electrical field amplitude when the optical field is transported from z_i to z_j.

Considering that RB and SpRS sources were distributed randomly along the entire fiber, integrating all the back reflections from locations z_i and z_2 along the fiber was inaccurate. To describe the randomness, we assumed that the locations of random scattering sources were uniformly distributed from 0 to L. Thus, in our simulation, we generated N points that were distributed uniformly from 0 to L. The N points were sorted by ascending counts, and the sorted sequence was $\{z_1, z_2, \cdots, z_k, \cdots z_{N-1}, z_N\}$, as illustrated in Fig. 3. In our model, the distributions of scattering sources were random. However, in other models, the scattering sources are distributed periodically since all the simulation step-lengths are set to be constant. Then, (2) can be rewritten as follows:

$$E_{DRB}(t) = \sum_{i=1}^{N}\sum_{j=1}^{i} T(z_j, z_i)\left[\gamma(z_j)\Delta z_j\right] T(z_i, z_j)\left[\gamma(z_i)\Delta z_i\right] \times T(0, L) E_{in}\left(t - nL/c - 2n(z_i - z_j)/c\right) \quad (3)$$

The terms $[\gamma(z_j)\Delta z_j]$ and $[\gamma(z_i)\Delta z_i]$ represent the reflectivity at z_i and z_j, respectively, in which $\Delta z_i = z_i - z_{i-1}, (i = 0, 1, \cdots, N)$ assuming $z_0 = 0$. In addition, $\gamma(z)$ was modeled as a complex white Gaussian zero-mean process [20]. Summarizing all possible DRB terms, we can obtain the total DRB electrical fields at the fiber output. Moreover, the total SpRS electrical fields at the fiber output can be expressed as follows:

$$E_{SpRS}(t) = \sum_{i=1}^{N} T(z_i, L)\varepsilon(z_i, t) \quad (4)$$

where $\varepsilon(z_i, t)$ is the total electrical field of the SpRS in the fiber section Δz_i. The electrical field varies randomly with time and locations, and the mean and variance of its amplitude are related to the pump power [19]. We assumed several different SpRS variations with pump power, and the optimized simulation results are shown in Section 3.

We solve the coupled intensity equations of Raman scattering [1], [6] as follows to obtain the transform function $T(z_i, z_j)$:

$$\begin{aligned}
\frac{dP_p^+}{dz} &= -\alpha_p P_p^+ - g_R \frac{\nu_p}{\nu_s} P_p^+ \left(P_s^+ + P_s^- + 4h\nu_s \Delta\nu\right) + \gamma_p P_p^- \\
\frac{dP_p^-}{-dz} &= -\alpha_p P_p^- - g_R \frac{\nu_p}{\nu_s} P_p^- \left(P_s^+ + P_s^- + 4h\nu_s \Delta\nu\right) + \gamma_p P_p^+ \\
\frac{dP_s^+}{dz} &= -\alpha_s P_s^+ + g_R \left(P_p^+ + P_p^-\right)\left(P_s^+ + 2h\nu_s \Delta\nu\right) + \gamma_s P_s^- \\
\frac{dP_s^-}{-dz} &= -\alpha_s P_s^- + g_R \left(P_p^+ + P_p^-\right)\left(P_s^- + 2h\nu_s \Delta\nu\right) + \gamma_s P_s^+
\end{aligned} \tag{5}$$

where $+$ and $-$ denote the forward and backward propagation of light in the fiber, respectively; P_p and P_s represent the pump power at frequency ν_p and the power of the amplified signal light at frequency ν_s, respectively; α_p and α_s are the attenuation coefficient for the pump light and signal light, respectively; and g_R is the Raman gain factor from the pump light to the signal light. The term $2h\nu_S\Delta\nu$ represents spontaneous Raman emission in the signal band, $\Delta\nu$ is the bandwidth of the signal light or the generated spontaneous radiation, and γ_p and γ_s are the Rayleigh backscattering coefficients for the pump light and signal light, respectively. We can calculate how the signal power changes along the fiber link, and the transform function of the electrical field amplitude can be written as

$$T\left(z_i, z_j\right) = \sqrt{\frac{P_s^+\left(z_j\right)}{P_s^+\left(z_i\right)}} \tag{6}$$

After we obtain the DRB and SpRS electrical fields at the fiber output, the total electrical field at the output of the fiber is

$$\begin{aligned}
E\left(t\right) &= E_s\left(t\right) + E_{DRB}\left(t\right) + E_{Sp}\left(t\right) \\
&= T\left(0, L\right) E_{in}\left(t - nL/c\right) + E_{DRB}\left(t\right) + E_{Sp}\left(t\right)
\end{aligned} \tag{7}$$

Finally, we employ a photonics detector (PD) to obtain the optical intensity and utilize a spectrum analyzer after the PD to acquire the spectrum of the total light intensity. The obtained spectrum can be represented by

$$\begin{aligned}
I\left(\omega\right) &= \mathbb{F}\left\{I\left(t\right)\right\} \\
&= \mathbb{F}\left\{\left(1/2\right)\varepsilon_0 nc\left|E\left(t\right)\right|^2\right\}
\end{aligned} \tag{8}$$

where $\mathbb{F}\{\bullet\}$ denotes the Fourier transform, and ε_0 is the vacuum permittivity.

3. Experiments and Analysis

We measured the spectra of the signal DRB and SpRS lights. Then, we compared the simulations based on our theoretical model with the experimental measurements. Our experimental setup to investigate the spectral characteristics of DRB noise is shown in Fig. 4. The light from an approximately 100 kHz linewidth laser at 1550 nm was fed into the fiber through a variable optical attenuator (VOA), which was used to adjust the launch power of the forward signal light. To avoid the spectrum distortion induced by optical nonlinear noise, the launch power was fixed at -7 dBm. Meanwhile, the forward and backward pump lights from two modules were coupled into the transmission fiber to provide distributed amplification. Both central wavelengths of the pump light were 1455 nm, and the pump power was 500 mW. The DRB and SpRS noise were generated along the fiber. Both signal and scattering noise were amplified in the transmission fiber. At the end of the fiber, we employed a fiber-delayed self-heterodyne interferometer to more precisely measure the received spectrum

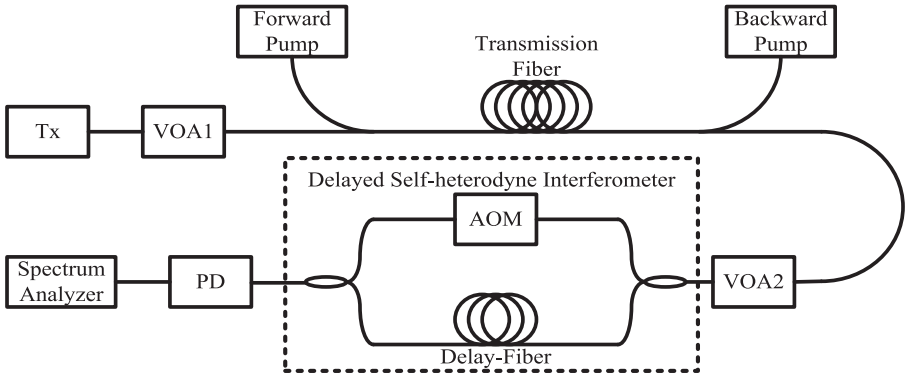

Fig. 4. Experimental setup for measuring the spectra of DRB and SpRS lights.

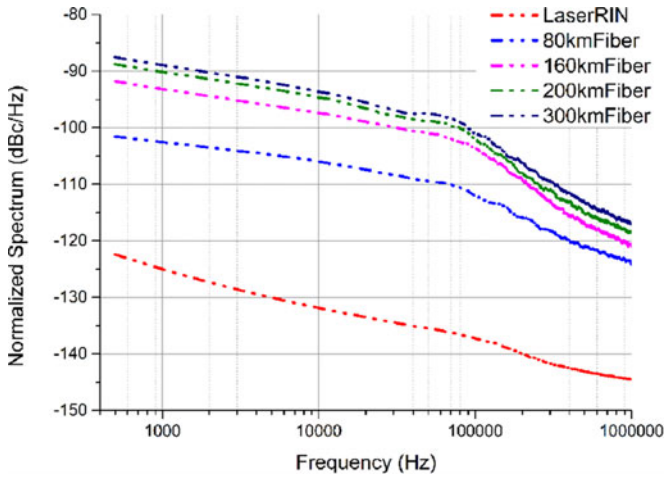

Fig. 5. Experimental measurements of the signal light spectra with DRB noise with different fiber lengths.

[21]. Before the fiber delayed self-heterodyne interferometer, another VOA was adopted to keep the optical power fed in the interferometer, which was fixed at the same value. The output light was split into two branches using a 3 dB optical coupler. The upper output was fed into an acousto-optic modulator (AOM), which generates a 40 MHz frequency shift. The lower output was delayed by time τ_d using a 20 km single-mode fiber. When the delayed time τ_d was much longer than the coherence time of the tested light, we obtained the spectrum of the light with high resolution [20]. Finally, the two branches of light were combined by another 3 dB optical coupler, which interfered with each other at the PD. We acquired the interference spectrum using an electrical spectrum analyzer after the PD. During the experiments, we measured the spectra of the DRB and SpRS noise with different fiber lengths such as 80 km, 160 km, 200 km, and 300 km. When the fiber length was 80 km, only the backward pump was on, while both pumps were on when the fiber lengths were 160 km, 200 km, and 300 km. The light power at the output of the transmission fiber was fixed at -18 dBm using VOA2.

In our simulation, the reference values of the parameters are shown as follows:

The experimental measurements of the signal and scattering noise spectra with different fiber lengths are shown in Fig. 5. The curves are the envelopes of the measured normalized spectra. The red dashed curve is the normalized spectrum of the laser relative intensity noise (Laser RIN). Fig. 5 demonstrates that the spectrum of light with DRB noise and corner frequency changed with the fiber length. In experiments conducted by M. Fleyer *et al.*, when the fiber length was longer, the

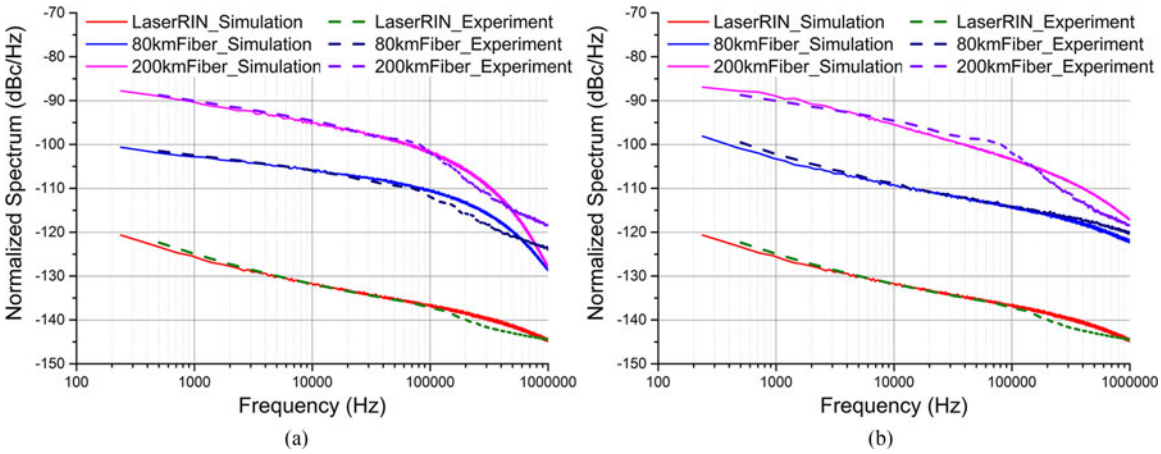

Fig. 6. Comparison of the signal lights' spectra with DRB noise between the experimental measurements and our simulations.

corner frequency was smaller in EDFA systems [19]. In our experiments, the corner frequency of an 80 km fiber was smaller than that of the other three fiber lengths. However, the corner frequencies of 160 km, 200 km, and 300 km fibers were not significantly different because the corner frequency approximately equals $f_c = c/2nL$ [19], [22]. In addition, due to the Raman amplification of the DRB light, the MPI noise was larger than that in the EDFA systems [19].

In Fig. 6(a), we compared the measurements and stimulations for 80 km and 200 km fibers. In the simulations in Fig. 6, we considered only the DRB noise and neglected the SpRS noise. The results of the simulations obviously agreed well with the experimental measurements in the low-frequency region. Since the MPI noise induced by DRB was a type of low-frequency noise, the comparisons proved that our theoretical model was accurate enough to describe the DRB noise in the distributed FRA systems.

In Fig. 6(b), we considered both the DRB and SpRS to simulate the received spectra. Clearly, the results of the simulation fit the experimental measurements better in the high-frequency region. In the high-frequency region, SpRS has a significant impact on the spectra. When we added a random SpRS to our model, the simulated results better fit the experimental results. However, when the fiber lengths were longer than 160 km, the simulated and experimental results were somewhat different at approximately 100 kHz. We attributed this difference to the fiber nonlinear effects. Since the Raman gain was extremely high, the signal peak power was sufficiently high to generate nonlinear effects, such as self-phase modulation and four-wave mixing between the pump and signal light. These nonlinear effects distorted the received spectrum. In future demonstrations, we will consider the fiber nonlinear effects in our theoretical model to improve the accuracy of the model in the high-frequency region.

4. Conclusion

In conclusion, to describe the randomness of scattering electrical fields with time and location, we proposed a precise random distribution theoretical model. Our theoretical model can accurately analyze the distributions and evolutions of the stochastic scattering along the fiber, which is meaningful for optimizing the performance of distributed fiber systems, especially systems with distributed amplification. In fiber communication systems that employ distributed FRAs, our theory can help adjust the pump configurations of FRAs to optimize the OSNR and expand the transmission distance. In OTDRs assisted by distributed amplification and random feedback fiber lasers, our model can also be used to analyze the system performance. In our further investigations, we will compare

our model with some existing techniques and known models in different fiber systems. And we will give more reliable and specific evidence to evaluate our model.

Acknowledgment

The authors would like to thank Dr. S. Yu and Dr. Q. Yang from Wuhan Research Institute of Posts and Telecommunications for their help.

References

[1] J. Bromage, "Raman amplification for fiber communications systems," *J. Lightw. Technol.* vol. 22, no. 1, pp. 79–93, Jan. 2004.
[2] W. S. Pelouch, "Raman amplification: An enabling technology for highcapacity, long-haul transmission," in *Proc. Opt. Fiber Commun. Conf.*, 2015, Paper W1C.1.
[3] D. Chang *et al.*, "150 x 120 Gb/s unrepeatered transmission over 409.6 km of large effective area fiber with commercial Raman DWDM system," *Opt. Exp.* vol. 22, no. 25, pp. 31057–31062, 2014.
[4] D. Chang *et al.*, "Unrepeatered 100G transmission over 520.6 km of G.652 fiber and 556.7 km of G.654 fiber with commercial Raman DWDM system and enhanced ROPA," *J. Lightw. Technol.* vol. 33, no. 3, pp. 631–638, Feb. 2015.
[5] V. Kalashnikov, S. V. Sergeyev, G. Jacobsen, S. Popov, and S. K. Turitsyn, "Multi-scale polarisation phenomena," *Light, Sci. Appl.*, vol. 5, Jan. 2016, Art. no. e16011.
[6] S. K. Turitsyn *et al.*, "Random distributed feedback fibre laser," *Nature Photon.* vol. 4, pp. 231–235, Feb. 2010.
[7] Y. Lu, T. Zhu, L. Chen, and X. Bao, "Distributed vibration sensor based on coherent detection of phase-OTDR," *J. Lightw. Technol.* vol. 28, no. 22, pp. 3243–3249, Nov. 2010.
[8] C. R. S. Fludger and R. J. Mears, "Electrical measurements of multipath interference in distributed Raman amplifiers," *J. Lightw. Technol.* vol. 19, no. 4, pp. 536–545, Apr. 2001.
[9] V. Kalavally, I. D. Rukhlenko, and M. Premaratne, "Combined effect of ASE and DRBS on noise in pulse-pumped fiber Raman amplifiers," *J. Lightw. Technol.* vol. 30, no. 18, pp. 2983–2987, Sep. 2012.
[10] F. Kong, J. Xue, R. H. Stolen, and L. Dong, "Direct experimental observation of stimulated thermal Rayleigh scattering with polarization modes in a fiber amplifier," *Optica*, vol. 3, no. 9, pp. 975–978, 2016.
[11] W. Wang *et al.*, "Amplified spontaneous emission and Rayleigh scattering in few-mode fiber Raman amplifiers," *IEEE Photon. Technol. Lett.*, vol. 29, no. 14, pp. 1159–1162, Jul. 2017.
[12] D. V. Churkin *et al.*, "Raman fiber lasers with a random distributed feedback based on Rayleigh scattering," *Phys. Rev. A*, vol. 82, no. 3, pp. 033828–033834, Sep. 2010.
[13] X. Du, H. Zhang, H. Xiao, P. Zhou, and Z. Liu, "Temporally stable random fiber laser operates at 1070 nm," *IEEE Photon. J.*, vol. 7, no. 5, Oct. 2015, Art. no. 1503107.
[14] H. F. Martins, S. M. López, P. Corredera, M. L. Filograno, O. Frazão, and M. G. Herráez, "Phase-sensitive optical time domain reflectometer assisted by first-order Raman amplification for distributed vibration sensing over $>$100 km," *J. Lightw. Technol.* vol. 32, no. 8, pp. 1510–1518, Apr. 2014.
[15] P. Gysel and R. K. Staubli, "Statistical properties of Rayleigh backscattering in single-mode fibers," *J. Lightw. Technol.* vol. 8, no. 4, pp. 561–567, Apr. 1990.
[16] P. Wan and J. Conradi, "Impact of double Rayleigh backscatter noise on digital and analog fiber systems," *J. Lightw. Technol.* vol. 14, no. 3, pp. 288—297, Mar. 1996.
[17] O. Okusaga, J. Cahill, A. Docherty, W. Zhou, and C. R. Menyuk, "Guided entropy mode Rayleigh scattering in optical fibers," *Opt. Lett.* vol. 37, no. 4, pp. 683–685, 2012.
[18] M. Fleyer, S. Heerschap, G. A. Cranch, and M. Horowitz, "Noise induced in optical fibers by double Rayleigh scattering of a laser with a 1/(f^ν) frequency noise," *Opt. Lett.* vol. 41, no. 6, pp. 1265–1268, 2016.
[19] C. Ottaviani *et al.*, "Creating single collective atomic excitations via spontaneous Raman emission in inhomogeneously broadened systems: Beyond the adiabatic approximation," *Phys. Rev. A* vol. 79, no. 6, pp. 063828–063833, Jun. 2009.
[20] Q. Feng *et al.*, "Investigations of backscattering effects in optical fibers and their influences on the link monitoring," *IEEE Photon. J.*, vol. 9, no. 2, Apr. 2017, Art. no. 7102009.
[21] M. van Deventer, "Polarization properties of Rayleigh backscattering in single-mode fibers," *J. Lightw. Technol.* vol. 11, no. 12, pp. 1895–1899, Dec. 1993.
[22] G. D. Domenico, S. Schilt, and P. Thomann, "Simple approach to the relation between laser frequency noise and laser line shape," *Appl. Opt.* vol. 49, no. 25, pp. 4801–4807, 2010.